


Effect of Solidification Processing Parameters and Silicon Content on the Dendritic Spacing and Hardness in Hypoeutectic Al-Si Alloys

Roberto Carlos Sales^a, Paulo Felipe Junior^a, Késsia Gomes Paradela^a,

Wysllan Jefferson Lima Garção^a, Alexandre Furtado Ferreira^{a*} 

^aPrograma de Pós-Graduação em Engenharia Metalúrgica, Universidade Federal Fluminense, 27255-125, Volta Redonda, RJ, Brasil

Received: May 08, 2018; Accepted: August 28, 2018

Aluminium with silicon as alloying element, form a class of material providing the most significant part of all material casting manufactured materials. These alloys have a wide range of applications in the automotive and aerospace industries. It is widely recognized that moderate addition of silicon to aluminum, significantly improves the resulting mechanical properties. Hypoeutectic Al-Si alloys were used in the present experimental study to investigate the solidification parameters effect and Si 3-5 wt% addition on the microstructural features and resulting hardness in a vertical directional solidification system. The hypoeutectic alloys were directionally solidified under transient heat flow conditions in a range of cooling rates from 0.3 to 4 °C/s. Characterization analyses by optical microscopy indicate clearly that secondary dendritic arm spacing (λ_2) increases significantly with the decrease in solidification speed (S_p) and cooling rate (\dot{T}). On the other hand, experimental growth laws relating the secondary dendritic arm spacing (λ_2) to the solidification speed (S_p) and cooling rate (\dot{T}) indicate that Si addition from 3 wt% to 5 wt% has induced a thickening effect leading to increase in λ_2 . While, experimental results have shown that the resulting hardness increase as solidification processing parameters (S_p and \dot{T}) increase. Results of Vickers hardness test for Al-5 wt% Si alloy has hardness increase of 18 % from that of Al-3 wt% Si alloy with mean values of 26 and 22 HV, respectively.

Keywords: *Al-Si alloys, unidirectional solidification, alloying elements, dendritic microstructure and microhardness.*

1. Introduction

Aluminium alloys with Si as the predominant alloying element have a wide range of applications in the automotive and aerospace industries due to an excellent combination of castability and mechanical properties, as well good corrosion resistance and wear resistivity. The more Si content an alloy contains, the lower is its thermal expansion coefficient. In hypoeutectic Al-Si alloy, the Si content varies from 5 to 12 wt%, the said solute is primarily responsible for so-called "good castability"; i.e., the ability to readily fill mold and to solidify castings with no hot tearing¹. Others alloying element as Cu and Mg are usually added to Al-Si alloys to improve the strength/weight ratio and enable the possibility of heat treatment¹⁻³. The microstructure developed throughout the solidification process contains α -Al dendrites as main constituent and can be decorated with eutectic Si particles³. It is well-known that the size, morphology and distribution of microstructural features have a significant role on the mechanical properties of these alloys, i.e., refined microstructure results in improved tensile properties^{4,5}. On the other hand, refinement of microstructure can be achieved through high cooling rate or chemical modification. Both the thermal parameters and solidification microstructure have been

considered in theoretical⁶⁻¹⁰ and experimental¹¹⁻¹⁸ works along the last decades. The effect of these process parameters on the quality of the final product has been of particular interest in the materials research field. Carvalho et al.⁸ used an Al-3 wt% Si alloy in order to investigate both the columnar to equiaxed transition (*CET*) and primary arm spacings (λ_1) in the horizontal directional solidification. Theoretical values of solidification speed, cooling rate (\dot{T}) and thermal gradient (G_L) obtained by these authors, were correlated with *CET* and λ_1 . The heat-transfer coefficient was experimentally calculated by Griffiths¹² during solidification process of Al-7 wt% Si in water-cooled system. The heat-transfer coefficients in the solidification vertically upward showed higher values than solidification vertically downward, while intermediate values was associated to horizontal solidification process. In these experiments, heat transfer during solidification is shown to be a phenomenon controlled by the surface roughness of the respective surfaces. The experimental results revealed that increasing the melt overheating temperature favors a less sensitive microstructure to cooling rate (\dot{T}) and solidification speed. An experimental study by Goulart et al.¹⁹, reported the thermal parameters effect on the resulting microstructure and mechanical properties of hypoeutectic Al-Si alloys. Experimental results obtained by Goulart et al.¹⁹, include secondary dendritic arm spacing, ultimate tensile strength and yield strength as a function of thermal parameters. It was found

*e-mail: alexandrefurtado@id.uff.br

that the ultimate tensile strength increases with decreasing secondary arm spacing, while the dendritic arrangement results illustrates no obvious effect on yield strength. Rodrigo et al.²⁰ have demonstrated the relationship between cooling thermal parameters, microstructural spacing and mechanical properties. Amongst results, as listed by the authors, refined globular Si particles seems to contribute for a combination of high tensile strength and elongation. Amongst results, as listed by the authors, refined globular Si particles seems to contribute for a combination of high tensile strength and elongation. It was shown by experimental results that the tensile properties increase significantly with the decrease in microstructural spacings. The analysis of the solidification processing parameters and solute additions is very important for the industrial solidification processes, due to its intrinsic correlation to the resulting microstructure and properties mechanical. It is in this general framework that the present experimental work is developed, highlighting the effects of the Si content (3 and 5 wt%) and solidification processing parameters, i.e., cooling rate (\dot{T}) and solidification speed (S_p) on the microstructural evolution and resulting hardness.

2. Experimental Procedure

Two binary hypoeutectic alloys (Al-Si), alloy-1 containing 3 wt% Si and alloy-2 containing 5 wt% Si, are prepared in an electrical resistance furnace at 750 °C, from commercial purity metals, i.e. 99.9 wt% Al, 99.7 %wt %Si. The casting assembly used in the directional solidification experiments is showed in details by Baptista et al.²¹, which consists of water-cooled mold with heat being extracted only from the bottom, promoting vertical upward directional solidification. Solidification experiments were performed with two hypoeutectic alloys (Al-Si) under thermally and solutally stable directional solidification conditions, i.e., natural convection due to density variations is not caused by temperature differences since the vertical casting is cooled from the bottom. The melts were poured into a steel mold, and then directionally solidified under transient heat flow conditions. A thin steel plate is used to close the base of the steel mold, which separates the melt from a water-cooling system. Both temperature of casting assembly and pouring were setup at 730 °C for both cases (alloy-1 and alloy-2). The water-cooling system was activated when thermal equilibrium was detected by data acquisition system. Along the solidification process, temperature was monitored by the output of a bank of type K thermocouples positioned at the central line of the castings at 5, 10, 15, 20, 35, 45, 60, 85 mm from the cooled bottom. The temperature was collected at intervals of 0.001 s, in order to permit an accurate determination of the cooling rate. The cooling rate (\dot{T}) has been calculated considering the temperatures vs. time data immediately after the passage of the liquidus isotherm for the different thermocouples positions in the casting. In order to

investigate the solidification processing parameters and alloy silicon content on dendritic morphology, microsegregation and hardness, samples were taken from locations close to the thermocouples tip along the castings (from 5 to 85mm). The selected transverse samples of the directionally solidified castings were polished and etched with a solution 0.5 % HF for metallography^{18,19}.

An Olympus Optical Microscope (Olympus Corporation, Japan) was used to produce digital images that were analyzed using the Goitaca (<https://sourceforge.net/projects/goitacaeq>) image processing software in order to measure the dendritic spacings. The schematic illustration of the secondary dendritic arm spacing (λ_2) measurements in the transverse sections are shown in Fig.1. It is important to remark that dendritic microstructures prevailed along the entire castings for any alloy experimentally examined. About 250-300 secondary dendritic arm spacing (λ_2) were measured for each specimen. The average dendritic arm spacing values were measured in the cross-section at least on four different regions for each specimen. The microhardness measurements were carried out at room temperature using Leitz Wetzlar Microhardness Tester. Measurements were made on the samples side surface using a Vickers pyramidal indenter with load and loading time equal to 200 g and 15 s, respectively. The microhardness values were the averages of least 10 indentations for each load.

3. Results and Discussion

Fig.2a-bshows cooling curve obtained experimentally under slow solidification, i.e., no water-cooled solidification system, with a cooling rate of about 0.47 °C/s. For the alloy-1 and alloy-2, solidification begins at liquidus temperature of 642 °C and 629 °C, respectively, as indicated by the change in the cooling curves caused by the release of latent heat. Upon the solidification completion, the slope of cooling curve alters again allowing the solidus temperature (T_s) to be determined.

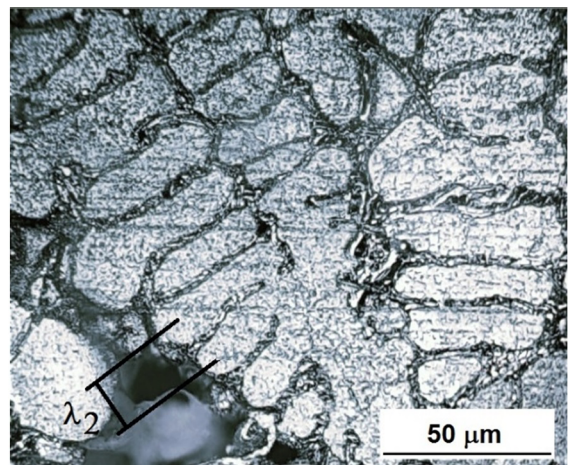


Figure 1. The schematic illustration of the secondary dendritic spacing (λ_2) measurements of Al-Si alloy.

Fig.3a-b shows the cooling curves determined for alloy-1 and alloy-2 during the solidification process under transient heat flow conditions in a water-cooled solidification setup. In this experiment, the thermocouples have been placed at different positions along the casting length. The temperature measurements for both alloys, are seen to decrease faster at regions closer to the water cooled bottom. The cooling rate gradually dwindles toward completion of local solidification. The numerical results of temperature versus time obtained by present work presents a similar behavior with those found in the literature, Carvalho et al.⁸, Griffiths¹² and Peres et al.¹⁵.

From Fig.3a-b, the position (P) of each thermocouple can be correlated with time (t) of passage of the liquidus temperature, thus permitting curves position of liquidus temperature (P) versus time (t) to be plotted, as shown in Fig. 4a-b.

The derivative of position of liquidus temperature as a function of time, permits that the solidification speed (S_p) as a function of time, to be determined, as showed in Tab. 1.

From experimental equations (P and S_p) shown in Table 1, it was possible to obtain an equation for the solidification speed (S_p) as a function of position, Fig. 5.

The relationship between solidification speed (S_p) and position (P) for both alloys is depicted in Fig.5, where the experimental results of both alloys, are plotted for comparison purposes. In both curves, the solidification speed (S_p) is seen to decrease faster at the onset of solidification, followed by a gradual decrease over time. This is due to the fact that water-cooling system favors higher solidification rate at the beginning of process, which decreases along the ingot because of the increasing thermal resistance of the solidified layer. One can see an appreciable deviation between the experimental curves,

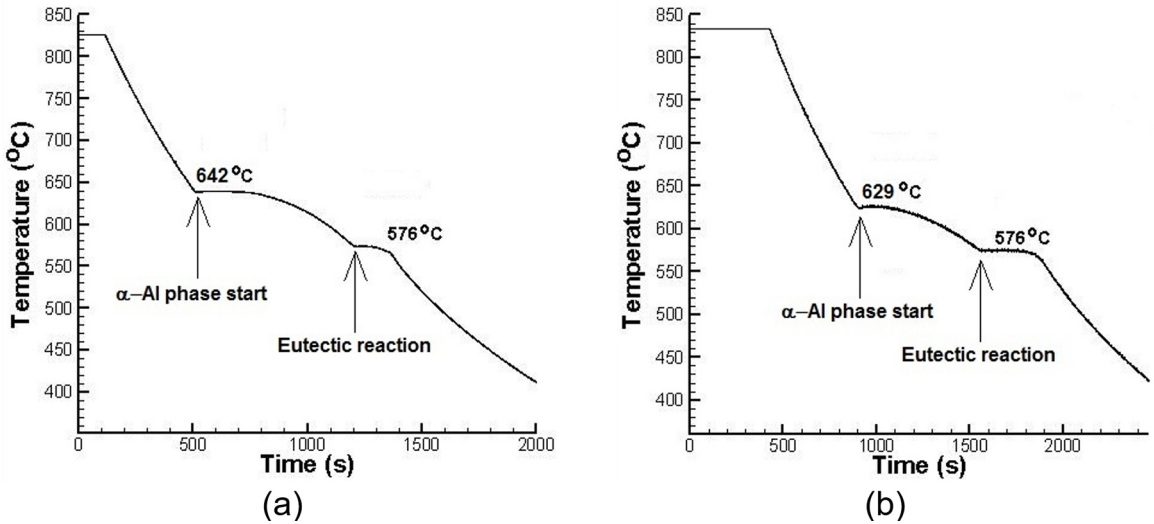


Figure 2 . Experimental cooling curves: (a) alloy-1 and (b) alloy-2.

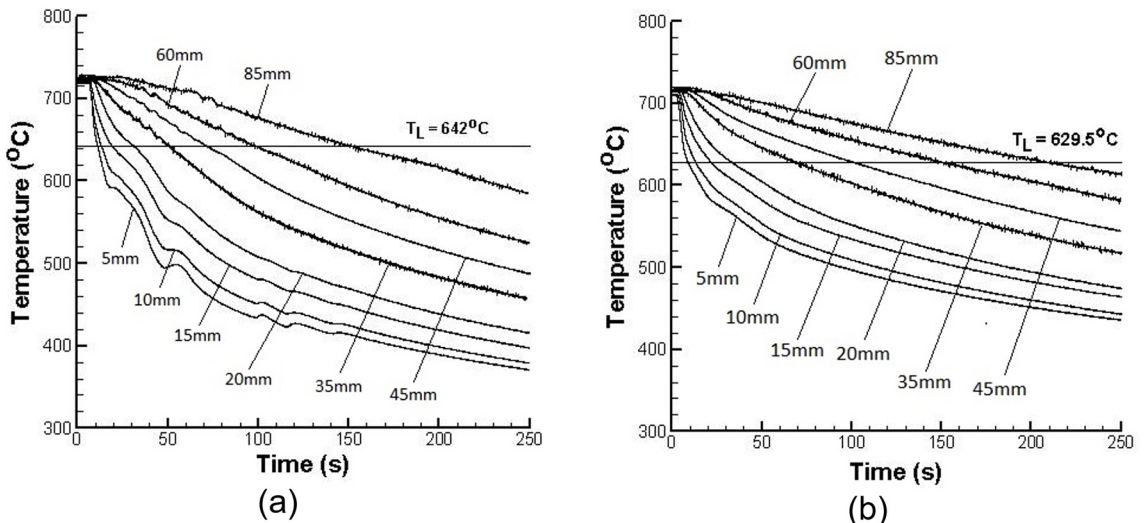


Figure 3 . Temperature versus time recorded at different positions along the length of the castings (a) alloy-1 and (b) alloy-2.

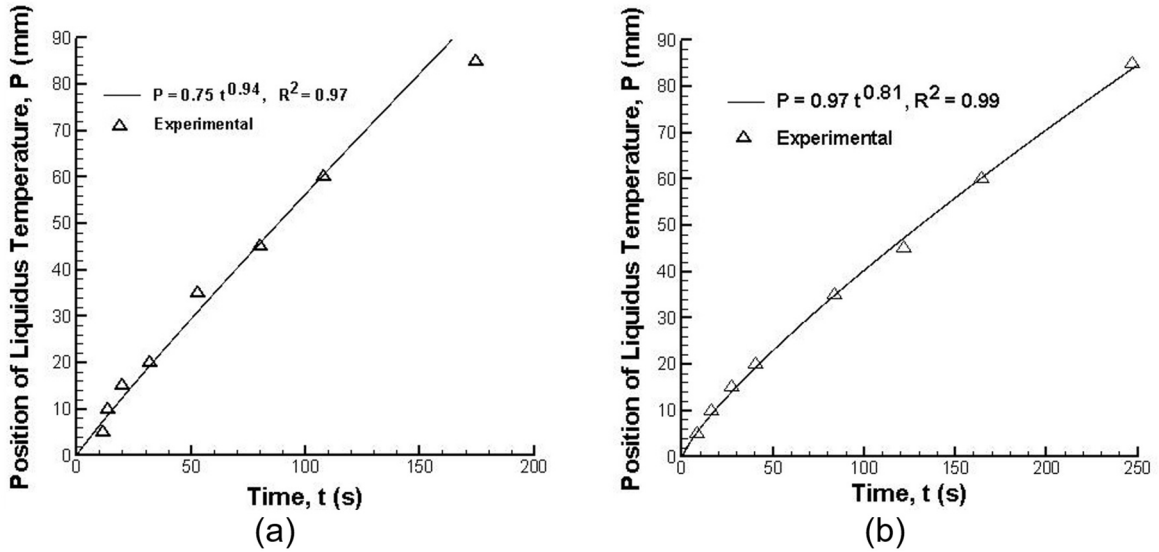


Figure 4. Position of liquidus temperature (P) versus time along the length of the castings: (a) alloy-1 and (b) alloy-2.

Table 1. Position of liquidus temperature and speed as a function time.

	Alloy-1	Alloy-2
Position as a function of time, $P=f(t)$	$P=0.75t^{0.94}$	$P=0.97t^{0.81}$
Speed as a function of time, $S_f=f(t)$	$S_f=0.71t^{0.06}$	$S_f=0.78t^{0.19}$

which indicates that the increase in the alloy silicon content from 3 to 5 wt% Si caused a decrease of solidification speed (S_p) along the casting length, Fig.5. As arguing previously, the solidification speed (S_p) is experimentally determined from data showed in Fig.3a-b. A quite complex dendritic arrangement prevailed along the entire length of castings, giving rise to a well-defined microstructure, as shown in Fig.6. In such dendritic networks, the secondary dendritic arms (λ_2) play an important role, since they contribute for a more extensive distribution of silicon solute (microsegregation) and of the intermetallics throughout the microstructure. It is worth noting that cooling rate (\dot{T}) and solidification speed (S_p) will also have an important role on solidification process, since they vary continuously along the casting length, and may affect microsegregation pattern and morphology dendritic. Fig.6 shows the microstructure evolution along the castings length of both examined alloys, at the right side of each photomicrograph, one can see information of sample position in the casting (P), solidification speed (S_p), cooling rate (\dot{T}) and secondary dendritic arm spacing (λ_2).

We can see that in both hypoeutectic Al-Si alloys the cooling rate (\dot{T}) decreases significantly along the castings length, Fig.7. High values of cooling rate (\dot{T}) at the base of the steel mold is due to water-cooling system. It was found significant deviations of experimental profiles between the alloys-1 and alloy-2 due to increasing solute content, from

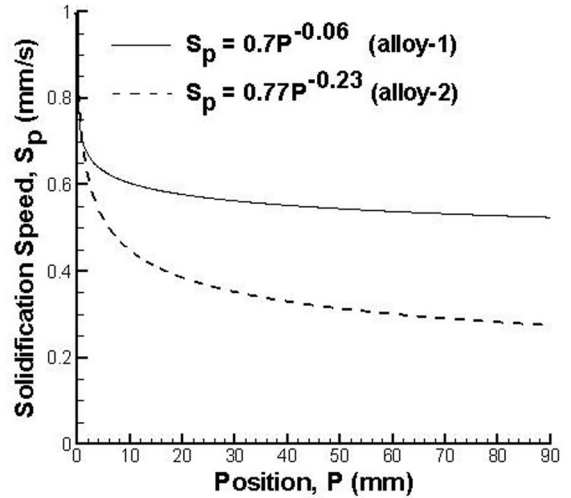


Figure 5. Solidification speed (S_p) versus position (P) along the casting length.

3 wt% to 5 wt% Si, in other words, the increasing of solute content exerts a strong influence on the said thermal variable.

It is interesting to highlight that Carvalho et al.⁸ and Peres et al.¹⁵, determined a numerical expression for both parameters thermal, solidification speed (S_p) and cooling rate (\dot{T}), which are similar to the showed in present work. However, both author's results lie above those obtained here, the difference is due to the several conditions of solidification process, such as the mold material, mold surface roughness, pouring temperature, mold pre-heating, etc. Next, the two curves in Fig.8 correspond to empirical equation for the alloy-1 and alloy-2. The focus of these results was on the dendritic arm spacing (λ_2) as a function of position (P) along castings. The dendritic arm spacing is seen to increase faster close to base of the steel mold, and then this increasing gradually diminishes towards completion of the solidification. However, as it can

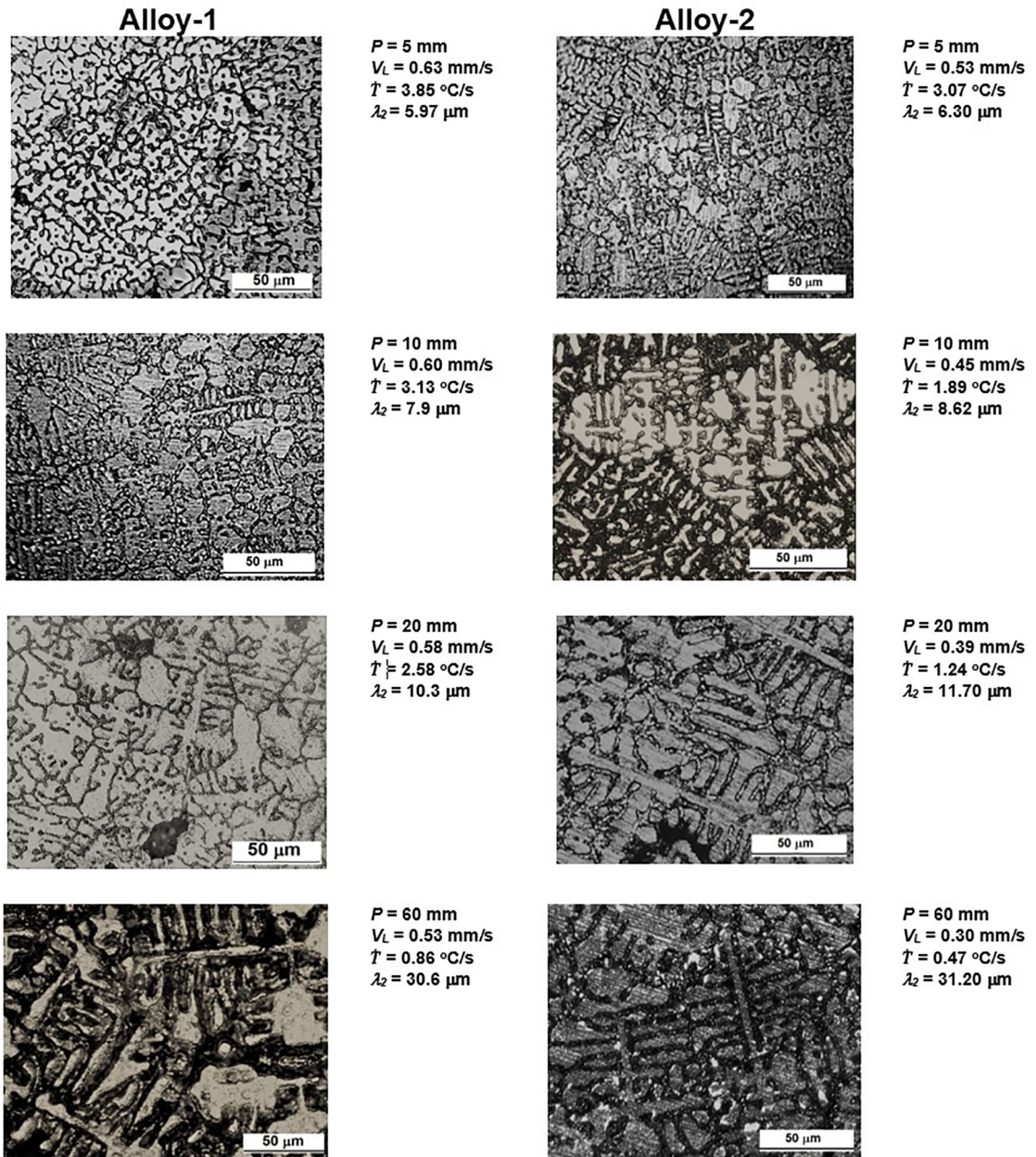


Figure 6 . Photomicrographs of samples taken from transverse sections along the castings.

be seen by increasing the silicon content in the alloy (from 3 wt% to 5 wt% Si), the dendritic arm secondary spacing suffered significant change.

In industrial solidification process, the most usual solid growth morphology is dendritic formation. A dendrite is an arrangement of primary, secondary, and occasionally higher degree branches, which results in an array where the spaces between the dendritic arms are occupied by eutectic or intermetallics phases. Investigations of the solidification speed and cooling rates in different positions along the ingots are of considerable importance in metallic alloys solidification

because said thermal parameters plays an important role on the both dendritic morphology and mechanical properties of cast products. Solidification speed (S_p) and cooling rate (\dot{T}) dependences on dendritic spacings (λ_2) are shown in Fig.9a-b, where the lines represent empirical power laws which fit the experimental points. The dendritic arm spacing variation with solidification speed for alloy-1 and alloy-2 are characterized by -1.8 and -0.9 power laws, respectively. While the dendritic spacing variation with cooling rate for alloy-1 and alloy-2 are characterized by -0.61 and -0.48 power laws. We can see that the dendritic spacing is influenced by

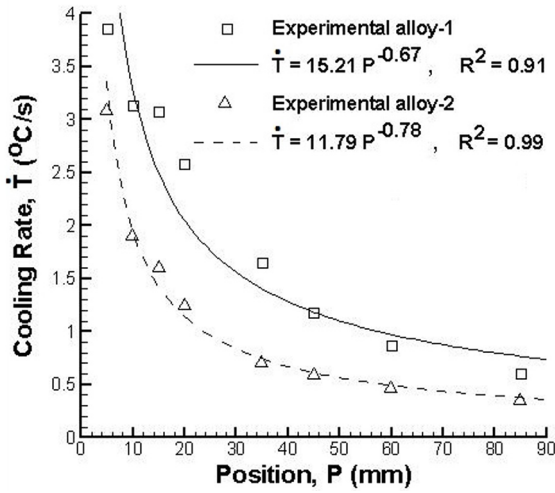


Figure 7. Cooling rate (\dot{T}) versus position (P) along the castings length.

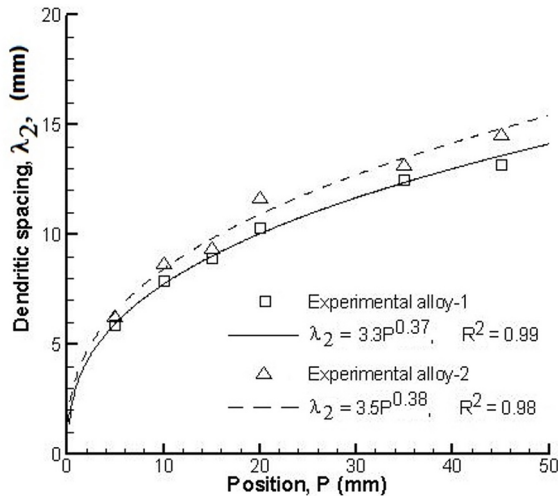
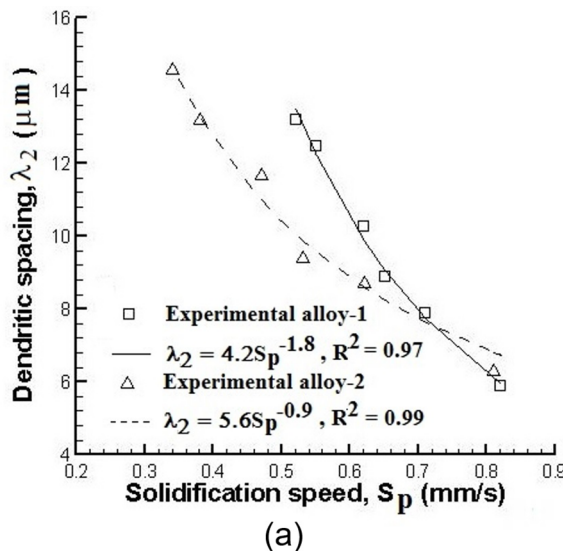
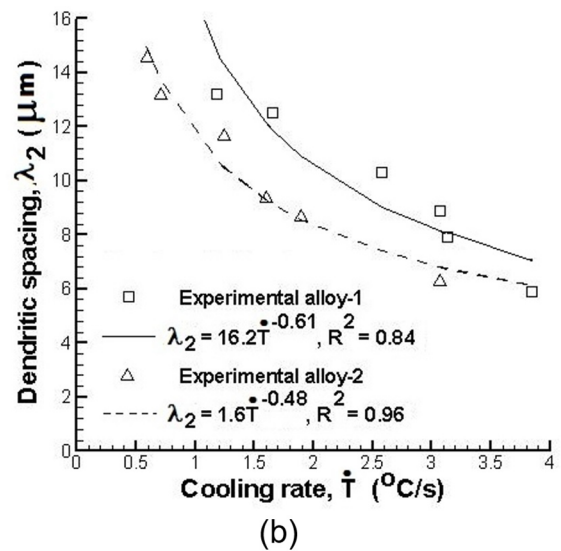


Figure 8. Secondary dendritic arm spacing (λ_2) versus position (P) along the castings length.



(a)



(b)

Figure 9. Dendritic spacing versus a) solidification speed (S_p) and b) cooling rate (\dot{T}).

the alloy solute content, which is evidenced by experimental laws representing dendritic arm spacing as a function either of solidification speed (S_p) or of cooling rate (\dot{T}).

Fig. 10 shows the hardness correlated with the thermal parameters, i.e., S_p and \dot{T} . According to these results, if the thermal parameters increases (S_p and \dot{T}) the hardness increases for both alloys investigated (alloy-1 and alloy-2). These parameters tend to increase at regions close to water-cooling system.

The heat flow conditions are key parameter in the control of the solidification of chill castings, and as a consequence, the resulting microstructure and hardness are also influenced by such conditions. In this sense, the mechanical properties are also influenced by microstructure. In order to examine these influences between the dendritic spacing and hardness, an equation has been derived from experimental results and is shown in Fig.11. The empirical equation established in Fig.11 permit to know the hardness of chill castings (alloy-1 and alloy-2) based on the dendritic arm spacing (λ_2).

The hardness increase with decreasing dendritic arm spacing. It is important to remark that a power function have been found to express such dependence. Low λ_2 values are typically found in regions close to the casting cooled surface. Dendrites characterized by smaller secondary arm spacings will have a more homogeneous distribution of the segregation and second phases during the solidification process. In addition, defects such as porosity are better distributed inside the castings, preventing the existence of preferential failing regions as a consequence of accumulation of defects². The understanding of the thermal parameters during the solidification can be used to gain insight into the chill castings.

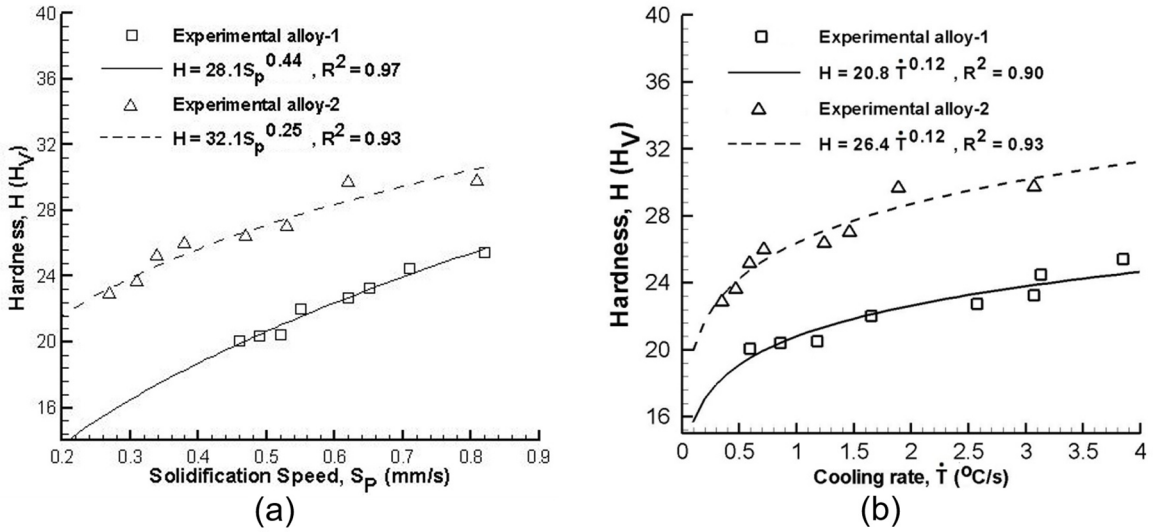


Figure 10 . Hardness versus a) solidification speed (S_p) and b) cooling rate (\dot{T}).

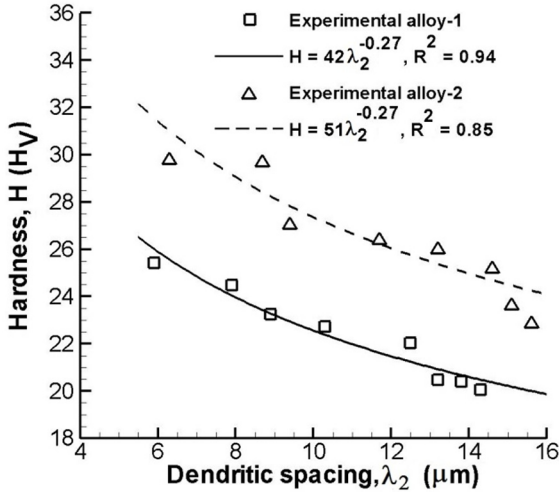


Figure 11 . Hardness (H) versus secondary dendritic arm spacing (λ_2).

4. Conclusions

The effect of solidification processing parameters (S_p and \dot{T}) and Si content on the secondary dendritic arm spacing (λ_2) and resulting hardness in hypoeutectic Al-Si alloys has been experimentally investigated. It was shown that increase in the alloy content from 3 to 5 wt% Si induces decrease in the solidification speed (S_p) and cooling rate (\dot{T}). However, if the content silicon increases the secondary dendritic arm spacing (λ_2) increases. The effects of the solidification speed and cooling rate on the secondary dendritic arm spacing has been examined by empirical power laws, which has been fitted to experimental points. In any case examined (alloy-1 and alloy-2) it has been shown that both thermal parameters have a significant role on the secondary dendritic arm spacing. The hardness can be correlated with these thermal parameters, which shown to vary according to a power function. It is

important to remark that hardness increases with addition of silicon (from 3 wt% to 5 wt% Si) in the aluminum alloy.

5. Acknowledgements

We would like to express our deep appreciation for the support provided by the Federal Fluminense University, for the use of their X-ray Microanalyses laboratories that allowed the development of the present study. Special thanks to the staff of these institutions that have greatly helped in the activities.

6. References

1. Davies JR, ed. *Aluminum and Aluminum Alloys*. Materials Park: ASM international; 1993.
2. Kapranos P, Kirkwood DH, Atkinson HV, Rheinlander JT, Bentzen JJ, Toft PT, et al. Thixoforming of an automotive part in A390 hypereutectic Al-Si alloy. *Journal of Materials Processing Technology*. 2003;135(2-3):271-277.
3. Ye H. An Overview of the development of Al-Si-Alloy based material for engine applications. *Journal of Materials Engineering and Performance*. 2003;12(3):288-297.
4. Chirita G, Stefanescu I, Soares D, Silva FS. Influence of vibration on the solidification behaviour and tensile properties of an Al-18 wt%Si alloy. *Materials & Design*. 2009;30(5):1575-1580.
5. Olofsson J, Svensson IL, Lava P, Debruyne D. Characterization and investigation of local variations in mechanical behaviour in cast aluminium using gradient solidification, Digital Image Correlation and finite element simulation. *Materials & Design (1980-2015)*. 2014;56:755-762.
6. Roland M, Kruglova A, Gaiselmann G, Brereton T, Schmidt V, Mücklich F, et al. Numerical simulation and comparison of a real Al-Si alloy with virtually generated alloys. *Archive of Applied Mechanics*. 2015;85(8):1161-1171.

7. Roland M, Kruglova A, Harste N, Mucklich F, Diebels S. Numerical Simulation of Al-Si alloys with and without a Directional Solidification. *Image Analysis & Stereology*. 2014;33(1):29-37.
8. Carvalho DB, Guimarães FC, Moreira AL, Moutinho DJ, Dias Filho JM, Rocha OL. Characterization of the Al-3wt.%Si alloy in unsteady-state horizontal directional solidification. *Materials Research*. 2013;16(4):874-883.
9. Guo D, Yang Y, Tong W, Hu Z. Numerical Simulation of Morphology and Microsegregation Evolution during Solidification of Al-Si Alloy. *Journal of Materials Science & Technology*. 2004;20(1):19-23.
10. Wu B, Jiang AL, Lu H, Zheng HL, Tian XL. Experimental Study and Numerical Simulation of Microstructure Evolution in Al-Si Eutectic Solidification Process. *Materials Science Forum*. 2018;913:212-219.
11. Griffiths WD, McCartney DG. The effect of electromagnetic stirring during solidification on the structure of Al-Si alloys. *Materials Science and Engineering: A*. 1996;216(1-2):47-60.
12. Griffiths WD. The heat-transfer coefficient during the unidirectional solidification of an Al-Si alloy casting. *Metallurgical and Materials Transactions B*. 1999;30(3):473-482.
13. Li P, Nikitin VI, Kandalova EG, Nikitin KV. Effect of melt overheating, cooling and solidification rates on Al-16wt.%Si alloy structure. *Materials Science and Engineering: A*. 2002;332(1-2):371-374.
14. Lu D, Jiang Y, Guan G, Zhou R, Li Z, Zhou R. Refinement of primary Si in hypereutectic Al-Si alloy by electromagnetic stirring. *Journal of Materials Processing Technology*. 2007;189(1-3):13-18.
15. Peres MD, Siqueira CA, Garcia A. Macrostructural and microstructural development in Al-Si alloys directionally solidified under unsteady-state conditions. *Journal of Alloys and Compounds*. 2004;381(1-2):168-181.
16. Radjai A, Miwa K, Nishio T. An investigation of the effects caused by electromagnetic vibrations in a hypereutectic Al-Si alloy melt. *Metallurgical and Materials Transactions A*. 1998;29(5):1477-1484.
17. Yilmaz F, Elliot R. The microstructure and mechanical properties of unidirectionally solidified Al-Si alloys. *Journal of Materials Science*. 1989;24(6):2065-2070.
18. Abu-Dheir N, Khraisheh M, Saito K, Male A. Silicon morphology modification in the eutectic Al-Si alloy using mechanical mold vibration. *Materials Science and Engineering: A*. 2005;393(1-2):109-117.
19. Goulart PR, Spinelli JE, Osório WR, Garcia A. Mechanical properties as a function of microstructure and solidification thermal variables of Al-Si castings. *Materials Science and Engineering: A*. 2006;421(1-2):245-253.
20. Reyes RV, Kakitani R, Costa TA, Spinelli JE, Cheung N, Garcia A. Cooling thermal parameters, microstructural spacing and mechanical properties in a directionally solidified hypereutectic Al-Si alloy. *Philosophical Magazine Letters*. 2016;96(6):228-237.
21. Baptista LAS, Ferreira AF, Paradelo KG, Silva DM, Castro JA. Experimental Investigation of Ternary Al-Si-Cu Alloy Solidified with Unsteady-State Heat Flow Conditions. *Materials Research*. 2018;21(3):e20170565.